Journal of Medical Systems (2019) 43: 275
https://doi.org/10.1007/s10916-019-1357-7

IMAGE & SIGNAL PROCESSING

Intervertebral Disc Segmentation and Diagnostic Application Based on Wavelet Denoising and AAM Model in Human Spine Image

Yang Yang[1] · Jian Wang[1] · Caie Xu[2]

Received: 11 March 2019 / Accepted: 22 May 2019 / Published online: 6 July 2019

Abstract
To solve the problem of location and segmentation of intervertebral discs in spinal MRI images, a method of intervertebral disc segmentation and degeneration classification diagnosis based on wavelet image denoising and independent component analysis-active appearance model (ICA-AAM) was proposed. Firstly, the spinal MRI image is decomposed by wavelet transform, and the noise is filtered by soft threshold method. Then, aiming at the inadequacy of PCA method in AAM in describing data details, ICA is used instead of PCA to model shape and texture models, and an improved AAM segmentation model is formed. Finally, the intervertebral discs in MRI images are segmented by AAM model, and the degeneration classification of intervertebral discs is diagnosed according to the gray level characteristics of the segmented region. The experimental results show that the method can accurately locate and segment the intervertebral disc region and make classification diagnosis.

Keywords Human spine MRI image · Image segmentation · Wavelet denoising · Active appearance model · Degeneration classification

Introduction

Spine-related diseases are a major problem facing modern human society. There is an urgent need for a computer-aided diagnosis and treatment system that can assist doctors in diagnosing spine diseases. Magnetic resonance imaging (MRI) is considered to be the most sensitive non-invasive spinal imaging modality. With the development of computer-assisted therapy in clinical diagnosis, more and more researchers began to devote themselves to computer analysis of magnetic resonance spinal images [1–4]. The accuracy of MRI image segmentation is very important for doctors to judge the real situation of the disease and make correct diagnosis.

At present, the methods for automatic location and segmentation of intervertebral discs mainly include two-level probability graph model based on pixel level and object level features, gradient histogram and support vector machine, model-based search methods, etc. For example, literature [5] considered prior information such as the relationship between adjacent intervertebral discs, and proposes a method of locating lumbar intervertebral discs based on two-level probability map model with pixel and object-level features, but the accuracy of location is not high and the effect of location is poor for diseased intervertebral discs. Literature [6] choose histogram of oriented gradients (HOG) as the feature to train, and divides the lumbar spine into two parts to locate, but it only relies on HOG, so the accuracy is not high. Literature [7] proposed a method of combining machine learning with probabilistic graph model. The pyramidal histogram of oriented gradients (PHOG) and image projection descriptor (IPD) are selected as local features of the image, and support vector machines (SVM) are used to classify each pixel point. Finally, the global optimal location results are obtained according to the second-order chain graph model. This method has high location accuracy, but the complexity of the algorithm is also

This article is part of the Topical Collection on *Image & Signal Processing*

✉ Yang Yang
yangyang201903@163.com

Caie Xu
G17DHL01@yamanashi.ac.jp

[1] Tongde Hospital of Zhejiang Province, Zhejiang 310012, Hangzhou, China

[2] Faculty of Engineering, University of Yamanashi, Kofu 4000016, Japan

large. At the same time, T1 and T2 images are needed. Literature [8] proposed a model-based method. Firstly, the vertebral curve was extracted by curve fitting, and then the intervertebral disc was located by template matching. This method does not use the information of adjacent intervertebral discs, and only the experimental results of 5 maps can't prove the reliability of the method.

Active appearance model (AAM) has been applied to medical image segmentation and registration, face feature extraction and other fields [9, 10]. AAM model builds shape model and texture model, and fuses them into appearance model that controls both shape and texture changes. AAM model combines the prior information of the image, and its model represents the average shape information of the image. At the same time, it combines the appearance information of gray and texture images to make its performance better than the active shape model (ASM). In the AAM, principal component analysis (PCA) is used to describe the details of the data. The purpose of PCA analysis is to extract the principal components of the shape and texture changes in training samples. The premise of PCA analysis is that the data of samples should obey multidimensional Gauss distribution [11–13]. However, in practice, not all training set data obey Gauss distribution, which will result in the inadequacy of PCA's ability to describe data details. The feature vectors generated by PCA analysis focus on describing the overall change of the object to be segmented, but when the weight parameters of the object to be change, the whole model will change, which will seriously affect the effect of segmentation [14].

Aiming at the inadequacy of PCA method used in AAM model in describing data details, independent component analysis (ICA) method is used to replace PCA method, and the shape and texture model is modeled to improve the ability of describing data details and form an improved AAM based on ICA. ICA-AAM model was used to locate and segment the intervertebral discs in the spinal MRI images, which was used to judge the degeneration of intervertebral discs and other pathological changes. The experimental results show that the proposed method can obtain clearer segmentation image, higher segmentation accuracy and better clinical diagnostic effect.

Wavelet image denoising

In the process of image formation, due to the influence of system equipment, some important information in the image is often polluted by noise, which adds difficulties to the correct analysis of the image, thus affecting the doctor's diagnosis. In order to obtain high quality images, it is necessary to denoise the MRI images. In this paper, the soft threshold method based on wavelet multi-scale decomposition is used to remove the noise of MRI image.

Wavelet decomposition

Wavelet transform is a method to describe multi-resolution space. Compared with Fourier transform, wavelet transform is a localized analysis of time (space) frequency. It refines the signal step by step through scaling translation operation, and finally achieves time subdivision at high frequency and frequency subdivision at low frequency. It can automatically adapt to the requirements of time-frequency signal analysis, thus focusing on arbitrary details of the signal [15, 16].

For any input signal $f(t)$, in function space $L^2(R)$, the constraint conditions are satisfied:

$$C_\phi = \int_R \frac{|\phi(\omega)|^2}{|\omega|} d\omega < \infty \tag{1}$$

$\phi(t)$ is a basic wavelet or mother wavelet, and the continuous wavelet transform is:

$$W_f(a,b) = \frac{1}{\sqrt{|a|}} \int_R f(t) \overline{\phi\left(\frac{t-b}{a}\right)} dt \tag{2}$$

It can be seen that continuous wavelet transform is the convolution of signal and wavelet function, and the wavelet function is in fact a filter of signal processing. The inverse transformation is:

$$f(t) = \frac{1}{C_\phi} \int_{R+} \int_R \frac{1}{a^2} W_f(a,b) \phi\left(\frac{t-b}{a}\right) da db \tag{3}$$

Through comparative analysis of experiments, the denoising effect is better when using coif2 wavelet base to decompose two layers. The image is decomposed and reconstructed by Mallat tower algorithm. The low-pass and high-pass filter coefficients provided by the wavelet filter. The signal through high-pass filter and low-pass filter, and the approximate low-frequency components (LL), Flat detail high frequency component (LH), vertical detail high frequency component (HL) and diagonal detail high frequency component (HH) are obtained.

Wavelet denoising

After an image is decomposed by wavelet transform, the high-frequency component represents the detail part and the noise part, and the low-frequency component represents the approximate part. Wavelet denoising is to remove the noise in high-frequency components. The commonly used denoising method is wavelet threshold denoising. The idea of threshold denoising method is to deal with the coefficients whose modulus is greater than or less than a threshold in each layer of coefficients after wavelet decomposition [17]. In threshold denoising, threshold functions reflect different processing strategies and estimation methods for wavelet decomposition

sparseness. The commonly used threshold functions are hard threshold function and soft threshold function.

Hard threshold function can preserve local features such as image edges, but the image will have pseudo-Gibbs effect. Soft threshold processing is relatively stable. Therefore, soft threshold method is adopted in this paper. The noise component is removed completely when the wavelet coefficient is smaller than the threshold value, and the signal component is the main component when the wavelet coefficient is larger than the threshold value, which is reserved after shrinking the amplitude. The threshold function is expressed as:

$$\hat{W}_{j,k} = \begin{cases} sign\left(W_{j,k}\right)\left(|W_{j,k}|-T\right), |W_{j,k}| \geq T \\ 0, |W_{j,k}| < T \end{cases} \quad (4)$$

Where, $W_{j,\ k}$ represents the wavelet coefficients, T represents the threshold, and $\hat{W}_{j,k}$ represents the new wavelet coefficients estimated by the soft threshold method.

Active appearance model (AAM)

AAM model is a shape and appearance model established after statistical learning of shape and texture of the object. It is obtained by adding texture training to the ASM method. The algorithm has a good effect on target extraction and good robustness. AAM model is a point distribution model (PDM), which uses finite marker points to approximate the shape of an object. Suppose an image uses n marker points to represent shape, and each marker point is two-dimensional, that is, n marker points contain $2n$ coordinate information. The shape of the target can be expressed by coordinate vectors as follows:$x = (x_1, y_1, x_2, y_2, \cdots, x_n, y_n)$.

In AAM, the samples are aligned by Euclidean distance calibration of shape vectors, and the texture vectors are standardized. The statistical models of shape and texture can be expressed as:

$$x = \overline{x} + P_s b_s, g = \overline{g} + P_g b_g \quad (5)$$

Where, $\overline{x}$ and $\overline{g}$ represent average shape and texture respectively. P_s and P_g are matrices composed of feature vectors of shape and texture respectively. b_s and b_g represent parameters of shape and texture model respectively. Principal Component Analysis (PCA) is used to analyze the shape and texture vectors in the samples, and a joint parameter b of shape and texture is obtained.

$$b = \begin{pmatrix} Wb_s \\ b_g \end{pmatrix} = \begin{pmatrix} Wb_s^T\left(x-\overline{x}\right) \\ P_g^T\left(g-\overline{g}\right) \end{pmatrix} \quad (6)$$

Where, W is a diagonal matrix with weights, which is used to balance the unit dimension difference between shape and texture coordinates. Through principal component analysis of joint parameters, the model of correlation between shape parameters and texture parameters can be obtained.

$$x = \overline{x} + Q_s c, g = \overline{g} + Q_g c \quad (7)$$

Where, Q_g and Q_s represent the texture and shape vectors in the joint model, and parameter c can control both the shape and texture parameters.

AAM's target search is an optimization process. By adjusting model parameter c and attitude parameter t, the difference between the image synthesized by the model and the image searched by the model is continuously reduced. Shape X in the image can be obtained by transforming x:$X = T_t(x)$. Similar to the shape in the image, the texture g_{im} in the image can also be obtained by transformation and offset adjustment: $g_{im} = T_u(g)$. where u is the adjustment parameter.

Model parameters c and t determine the shape and position of the model in the image frame. In the matching process, the image on shape X is cut down to get sample g_{im}, and then the sample is projected into the normalized space by the inverse transformation of T_u:$g_s = T^{-1}(g_{im})$, and then compared with the texture g_m produced by the model. Therefore, the error between the current model and the target can be expressed as [18–20]:

$$r(p) = g_s - g_m, p^T = \left(c^T|t^T|u^T\right) \quad (8)$$

The aim of AAM search optimization is to minimize the error $E(p) = r^T r$, so the root mean square solution can be obtained.

$$\partial p = -Rr(p) \quad (9)$$

Where, $R = \left(\frac{\partial r^T}{\partial p}\frac{\partial r}{\partial p}\right)^{-1}\frac{\partial r^T}{\partial p}$. The search process of AAM is to repeat the algorithm steps until the error r is not reduced.

Image segmentation based on ICA-AAM model

In the AAM model, PCA method is used to describe the details of the data in order to extract the principal components of the shape and texture changes in the training samples.

Firstly, the target object in all training samples is calibrated manually. Procrustes analysis is used to align the calibration points of the samples, eliminating the translation, rotation, scaling and other factors between samples, and then the two-dimensional point distribution model (PDM) of the target object is obtained. Using PCA to analyze aligned samples, the shape model is obtained.

$$s = \overline{s} + P_s b_s \quad (10)$$

Where, $\overline{s}$ is the average shape vector, P_s is a matrix consisting of covariance eigenvectors of all calibration points., and b_s is the shape model vector, which contains the weight of each eigenvector. The shape change of the model is controlled by changing b_s.

Similar shape model is established. Through gray sampling of calibrated samples, one-to-one texture samples corresponding to the pixels in the training set are obtained. Alignment and normalization of texture, and then PCA analysis to get texture model:

$$t = \overline{t} + P_t b_t \tag{11}$$

In the formula, $\overline{t}$ is the average texture vector, P_t is the matrix composed of feature vectors, and b_t is the texture model vector, which controls the texture change of the model.

The appearance model is obtained by fusing shape and texture models. After unifying the parameters of the two models and PCA analysis, the appearance model is finally formed.

$$a = \overline{a} + P_a b_a \tag{12}$$

In the formula, $\overline{a}$ is the average appearance model vector, P_a is the feature matrix, and b_a can control the change of shape and texture at the same time.

PCA analysis aims to extract the principal components of shape and texture changes in training samples. Its premise is that the sample data must obey the multi-dimensional Gauss distribution. However, in many practical applications, the training data do not all obey this distribution model. At the same time, the feature vectors generated by PCA analysis focus on describing the overall change of the object to be segmented. When the weight parameters of the object are changed, the whole model will change. In addition, PCA needs the data of samples to obey the multi-dimensional Gauss distribution. In practice, not all the data of training sets obey the Gauss distribution, which results in the inadequacy of PCA's ability to describe the details of data. Aiming at the inadequacy of PCA method in describing data details, Uzlimcii [21] replaces PCA method with ICA method. An active appearance model (ICA-AAM) based on independent component analysis (ICA-AAM) is proposed, which is applied to ventricular segmentation in cardiac MRI and achieves better segmentation results.

In this paper, seven vertebral bodies of T12-S1 in T2-weighted images are segmented accurately, and quantitative analysis of degenerative changes of intervertebral discs is carried out based on this. Although the shape of lumbar intervertebral disc in MRI is similar, its shape and texture are different due to individual differences. Its shape and texture model are difficult to obey multi-dimensional Gauss distribution. PCA-AAM segmentation will inevitably lead to large errors. ICA-AAMs was introduced to segment intervertebral discs.

Independent component analysis (ICA), also known as blind signal separation, is an extension of second-order statistical analysis to higher-order statistical analysis, and is widely used in mixed signal separation. Taking shape model as an example, ICA can be expressed as:

$$X = A \cdot S \tag{13}$$

Where, $X = (x_1, x_2, \cdots, x_m)^T$ represents the m-dimensional shape vector, A is the mixed matrix of $m \times m$, $S = (s_1, s_2, \cdots, s_n)^T$ represents the n-dimensional source signal vector, whose components are independent of each other. The purpose of blind source separation is to decompose the shape vector X to be analyzed into statistically independent components by some linear transformation.

$$\hat{S} = UX \tag{14}$$

Where, $\hat{S}$ is the estimated vector of S, which is called independent component (IC), and U is the unmixing matrix. The joint approximative diagonalization of eigen matrix (JADE) algorithm with strong robustness is used to solve U, so that the non-Gaussian property of $\hat{s}_k$ in $\hat{S} = (\hat{s}_1, \cdots, \hat{s}_n)^T$ is maximized.

PCA ranks the separated principal components according to their variances from large to small, while ICA algorithm itself does not rank the separated independent components. In most cases, the sorting of source signals has little effect on the problems considered, but this work needs to determine the sorting order of independent components. A method of sorting based on the deviation of independent component modulus is proposed. For example, formula (15) and formula (16), according to the deviation between the modulus of each independent component and the average modulus, the independent components are sorted. First, the modulus $M_i (i = 1, \cdots, n)$ of each independent component is calculated, and then the average $\overline{M}$ of each independent component is calculated.

$$M_i = \sqrt{\sum_{k=1}^{n} (s_{ik})^2} \tag{15}$$

$$\overline{M} = \frac{1}{n} \sum_{i=1}^{n} M_i \tag{16}$$

Where, s_{ik} is the k-th element in the i-th independent component. The deviation $r = |M_i - \overline{M}|$ between the modulus of each independent component with the average modulus are calculated and sorted according to its value from large to small. Experiments show that this sort method is effective and easy to calculate.

When building ICA-AAMs model, the gray distribution of vertebral body and adjacent soft tissues in waist T2-weighted images varies greatly. ICA analysis of shape and texture information will make the final appearance model describe

details more fully. Therefore, in this work, both shape model and texture model are generated by ICA.

ICA-AAM algorithm flow is as follows:

Step 1: Initialize all the components of the parameter vector: model parameter c_0, attitude parameter t_0, texture parameter u_0, let $p = p_0$, and get the average shape, average texture and average length information of the model by ICA method.

Step 2: Calculate the error r between the model and the target.

Step 3: Calculate the length D of the contour points obtained in the matching process, and calculate the error d between the contour points and the corresponding model points.

Step 4: Calculate the current error $E(p)$;

Step 5: Set vector adjustment parameter $K = 1$;

Step 6: Update parameter vector $\hat{p} = p + K\partial p = p - KRr$;

Step 7: Calculate the new error vector $\hat{r}$ with the updated parameter vector $\hat{p}$.

Step 8: If $\|\hat{r}\|^2 < E$, the new parameter is$p = \hat{p}$ and the algorithm terminates..

Step 9: Otherwise, let $K = 1.5$, $K = 0.5$, $K = 0.25$ et al. continue step 6 until error r is no longer reduced. Where, the value of $K$is set according to the analysis of many test results.

Experiment and analysis

Experimental setup

Lower back pain (LBP) as the most common form of spinal disease, has become a research hotspot in the field of image processing. At present, it is generally believed that the cause of LBP is related to the degeneration of intervertebral disc. In this experiment, the region of intervertebral disc will be located and segmented through the process of MRI image processing, and the degree of degeneration will be graded by SVM classifier according to the gray characteristics of intervertebral disc.

In T2-weighted images of MRI, Pfirrmann classified the degeneration of lumbar intervertebral disc into five grades according to the structure of nucleus pulposus, the boundary between nucleus pulposus and annulus fibrosus, signal intensity and the height of intervertebral disc, as shown in Fig. 1.

Grade 1: The structure of the intervertebral disc is uniform white high signal, and the height of the intervertebral disc is normal.

Grade 2: The structure of the intervertebral disc showed uneven white high signal; the difference between annulus fibrosus and nucleus pulposus was obvious.

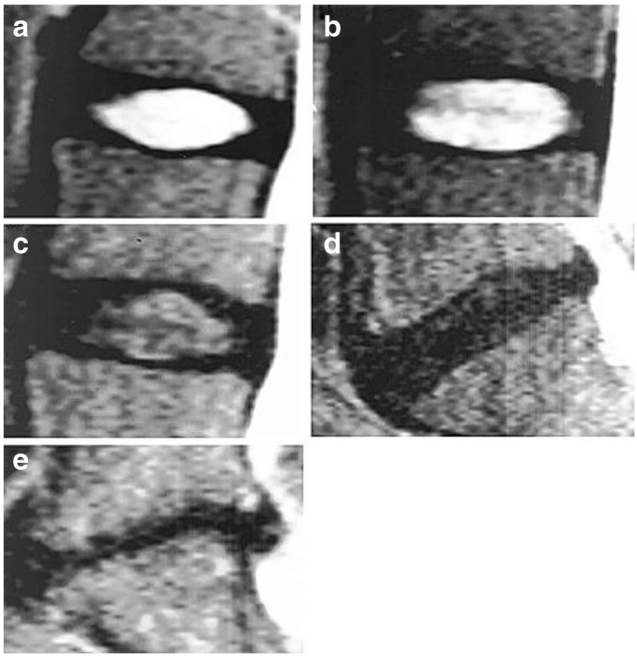

Fig. 1 An illustration of Pfirrmann disc degeneration classification

Grade 3: the signal intensity of the structure of the intervertebral disc was uneven, and the signal intensity in the middle is gray; the difference between annulus fibrosus and nucleus pulposus was not obvious, and the height of the intervertebral disc was normal or slightly decreased.

Grade 4: the intervertebral disc The signal of disc structure is uneven, showing black low signal; the difference between nucleus pulposus and annulus fibrosus disappears, and the height of intervertebral disc decreases normally or moderately.

Grade 5: the signal of disc structure is uneven, showing black low signal; the difference between nucleus pulposus and annulus fibrosus disappears, and the intervertebral space collapses.

Tests were performed on T2-weighted image datasets of 32 patients. The repetition time (TR) and echo time (TE) are between 3000 and 4000 ms and 112–121 ms, respectively. The image size is 512 × 512 pixels. The image data set contains 225 intervertebral discs. Each intervertebral disc is graded by experts. It contains 10 images of grade 1, 25 images of grade 2, 90 images of grade 3, 82 images of grade 4 and 18 images of grade 5. The partitioning program is realized by MATLAB programming.

Performance indicators

Sensitivity (also known as true positive rate), specificity (also known as true negative rate) and accuracy (Accuracy) were used to evaluate the grading results, which were defined as

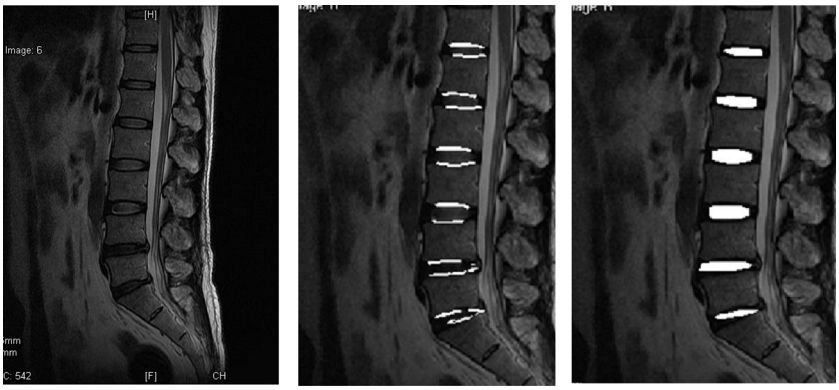

(a) spinal MRI image (b) Location boundary of intervertebral disc (c) Segmented intervertebral disc region

Fig. 2 Intervertebral Disc Segmentation in Spinal MRI Images

follows:

$$\text{Sensitivity} = TP/(TP + FN) \tag{17}$$

$$\text{Specificity} = TN/(TN + FP) \tag{18}$$

$$\text{Accuracy} = (TP + TN)/(TP + TN + FN + FP) \tag{19}$$

Where, *TP*, *TN*, *FP* and *FN* were true positive, true negative, false positive and false negative respectively. In this experiment, these performance parameters are obtained by comparing the results of automatic classification with those of expert classification. The higher the sensitivity of diagnostic test, the lower the rate of missed diagnosis. The higher the specificity, the lower the rate of misdiagnosis.

Result analysis

Firstly, the proposed segmentation method is implemented. An example of segmentation is given in Fig. 2. It can be seen that this method can accurately locate and segment the intervertebral disc region from the vertebral MRI images, which provides favorable conditions for the subsequent classification of degeneration according to the characteristics of the segmented intervertebral disc region.

In the experimental data set, 60% of them are used as training images to construct the proposed ICA-AAM model, and the remaining 40% are used as test images. In order to prove the validity of ICA-AAM, this paper compares it with the traditional AAM model, and the classification results are shown in Table 1. The experimental data were the average of five experiments.

It can be seen that the ICA-AAM model used in this paper obtains 87.5% accuracy in disc degeneration classification recognition, while the traditional AMM model only obtains 81.2% accuracy, which proves the effectiveness of ICA-AAM model. This is because in the traditional AAM model, the PCA method is used to describe the details of the data in order to extract the principal components of the shape and texture changes in the training samples. But it needs the data of samples to obey the multi-dimensional Gauss distribution. In practice, not all the data of training sets obey the Gauss distribution, which results in the inadequacy of PCA's ability to describe the details of data. The similarity between ICA and PCA is that both of them seek a feature space from the original sample data, and then map the new data to the feature space to obtain a set of feature vectors for classification and recognition. The difference is that ICA algorithm requires each component to be statistically independent or as independent as possible, while PCA is not. Therefore, ICA-AAM model has better separability.

Table 1 Grading diagnosis of intervertebral disc degeneration using this method

	performance index	Grade 1	Grade 2	Grade 3	Grade 4	Grade 5	weighted mean
ICA-AAM	Sensitivity (%)	83.25	86.83	89.42	82.06	92.44	86.41
	Specificity (%)	92.45	90.76	86.53	89.97	92.69	89.01
	Accuracy (%)	91.42	88.59	87.38	86.04	91.42	87.53
AAM	Sensitivity (%)	79.43	84.53	79.94	76.83	86.27	79.80
	Specificity (%)	85.85	82.82	82.62	83.64	82.67	83.16
	Accuracy (%)	84.13	83.91	81.35	79.04	85.38	81.24

Table 2 Grading diagnosis of intervertebral disc degeneration by various methods

method	Sensitivity (%)	Specificity (%)	Accuracy (%)
literature [6]	78.35	80.61	79.93
literature [7]	84.82	82.75	84.02
Proposed method	86.41	89.01	87.53

This method is compared with several existing methods, which are based on the histogram of oriented gradients (HOG) proposed in literature [6], and based on machine learning and probability graph model proposed in literature [7]. In order to make a fair comparison, after locating and segmenting the intervertebral disc region, SVM is used to classify the degeneration based on gray features. The classification results of various methods are shown in Table 2.

It can be seen that the performance of literature [7] method is higher than that of literature [6]. This is because the method of literature [6] only relies on HOG as its feature, while the method of literature [7] chooses pyramidal histogram of oriented gradients (PHOG) and image projection descriptor (IPD) as its local feature, which improves the accuracy of localization to a certain extent. The proposed method achieves the highest performance because it uses the model-based method to construct shape model and texture model through ICA analysis, which is used to locate and segment the intervertebral disc region and achieves high accuracy.

Conclusion

In this paper, a new method of intervertebral disc segmentation and degeneration classification diagnosis based on wavelet image denoising and ICA-AAM model is proposed. ICA is used instead of PCA to model the shape and texture model, which improves the ability of describing the details of data. The ICA-AAM model is constructed to segment and classify the intervertebral discs in MRI images. Compared with traditional AAM, this method improves the accuracy of segmentation, achieves a more accurate classification of 5 grades of degeneration, and is better applied in clinical diagnosis. In addition, the framework can continue to extract and analyze other lumbar physiological parameters quantitatively.

Compliance with Ethical Standards

Conflict of Interest We declare that we have no conflict of interest. This article does not contain any studies with human participants or animals performed by any of the authors. Informed consent was obtained from all individual participants included in the study.

References

1. Ghosh, S. , Alomari, R. S. , and Chaudhary, V. et al., Computer-aided diagnosis for lumbar mri using heterogeneous classifiers[C]// IEEE international symposium on biomedical imaging: From Nano to macro. IEEE, 2011.
2. Oktay, A. B., Albayrak, N. B., and Akgul, Y. S., Computer aided diagnosis of degenerative intervertebral disc diseases from lumbar MR images[J]. *Comput. Med. Imag. Graph. Off. J. Comput. Med. Imag. Soc.* 38(7):613–619, 2014.
3. Alomari, R. S., Corso J J , Chaudhary V , et al. toward a clinical lumbar CAD: Herniation diagnosis[J]. *Int. J. Comput. Assist Radiol. Surg.* 6(1):119–126, 2011.
4. Marcelo, D. S. B. , Nogueirabarbosa, M. H. , Rangayyan, R. M. ,et al., Semiautomatic classification of intervertebral disc degeneration in magnetic resonance images of the spine[C]// Biosignals & Biorobotics Conference. IEEE, 2014.
5. Alomari, R. S., Corso, J. J., and Chaudhary, V., Labeling of lumbar discs using both pixel- and object-level features with a two-level probabilistic model[J]. *IEEE Trans. Med. Imag.* 30(1):1–10, 2011.
6. Ghosh, S., and Chaudhary, V., Supervised methods for detection and segmentation of tissues in clinical lumbar MRI[J]. *Comput. Med. Imag. Graph.* 38(7):639–649, 2014.
7. Oktay, A. B., and Akgul, Y. S., Simultaneous localization of lumbar vertebrae and intervertebral discs with SVM-based MRF[J]. *IEEE Trans. Biomed. Eng.* 60(9):2375–2383, 2013.
8. Peng, Z., Zhong, J., and Wee, W., et al., Automated vertebra detection and segmentation from the whole spine MR images[C]//. International conference of the engineering in Medicine & Biology Society. IEEE, 2006.
9. Chen, X., Udupa, J. K., Bagci, U. et al., Medical image segmentation by combining graph cuts and oriented active appearance models[J]. *IEEE Trans. Image Process. Publ. IEEE Signal Process. Soc.* 21(4):2035, 2012.
10. Gao, X., Su, Y., Li, X. et al., A review of active appearance models[J]. *IEEE Trans. Syst. Man Cybernet. Part C Applic. Rev.* 40(2):145–158, 2010.
11. Toth, R., and Madabhushi, A., Multifeature landmark-free active appearance models: Application to prostate MRI segmentation[J]. *IEEE Trans. Med. Imag.* 31(8):1638–1650, 2012.
12. Inamdar, R. S., and Ramdasi, D. S., Active appearance models for segmentation of cardiac MRI data[C]// international conference on communications and signal processing. IEEE. 96–100, 2013.
13. Sapthagirivasan, V., Anburajan, M., and Mahadevan, V., Segmentation of proximal femur in digital radiographic image using principal component model[C]//. International conference on electronics computer technology. IEEE, :113–117, 2011.
14. Yu, W., Face recognition using constrained active appearance model[C]//. International Symposium on Intelligent Information Technology Application Workshops. IEEE :348–351, 2010.
15. Deng, G., and Liu, Z., A Wavelet Image Denoising based on the new threshold function[C]// international conference on computational intelligence and security. IEEE :158–161, 2016.
16. Saluja, R., and Boyat, A., Wavelet based image denoising using weighted highpass filtering coefficients and adaptive wiener filter[C]//. International Conference on Computer, Communication and Control. IEEE, :1–6, 2016.
17. Ismael, S. H., Mustafa, F. M., and Okümüs, I. T. A., New approach of image Denoising based on discrete Wavelet transform[C]// computer applications & research. IEEE :36–40, 2016.
18. Itakura, H., Achrol, A. S., Mitchell, L. A. et al., Magnetic resonance image features identify glioblastoma phenotypic subtypes with distinct molecular pathway activities[J]. *Sci. Translat. Med.* 7:303, 2015.

19. Raskolnikov, D., George, A. K., Raisbahrami, S. et al., The role of magnetic resonance image guided prostate biopsy in stratifying men for risk of extracapsular extension at radical prostatectomy.[J]. *J. Urol.* 194(1):105–111, 2015.
20. Duan, G., Sawant, N., and Wang, J. Z., et al., Analysis of cypriot icon faces using ICA-enhanced active shape model representation[C]//. ACM International Conference on Multimedia. ACM, :901–904, 2011.
21. Üzümcü, M., Frangi, A. F., and Sonka, M., et al., ICA vs. PCA active appearance models: Application to cardiac MR segmentation[C]// Medical image computing and computer-assisted intervention - Miccai 2003, international conference, Montréal, Canada, November 15–18, 2003, proceedings. DBLP, 2003:451–458, 2003.